



## Performance and theoretical study on corrosion inhibition of new Triazolo-pyrimidine derivative for Carbon steel in hydrochloric acid

Y. El Bakri<sup>1,\*</sup>, M. Boudalia<sup>2</sup>, S. Echih<sup>2,3</sup>, A. Harmaoui<sup>1</sup>, J. Sebhaoui<sup>1</sup>, H. Elmsellem<sup>4</sup>,  
A. Ben Ali<sup>6</sup>, Y. Ramli<sup>5</sup>, A. Guenbour<sup>2</sup>, A. Bellaouchou<sup>2</sup>, E.M. Essassi<sup>1</sup>

<sup>1</sup>Laboratoire de Chimie Organique Heterocyclique, URAC 21, Pôle de Compétences Pharmacochimie, Université Mohammed V, Faculté des Sciences, Av. Ibn Battouta, BP 1014 Rabat, Morocco

<sup>2</sup>Laboratory of Materials, Nanotechnology and Environment, Faculty of Science, Mohamed V University in Rabat Av. Ibn Battouta, BP 1014 Rabat, Morocco.

<sup>3</sup>Laboratory of Water and Environment, Faculty of Sciences of El jadida, BP 20, 24000 El jadida, Morocco

<sup>4</sup>LCM2AE, Faculté des Sciences, B.P. 717, 60000 Oujda, Morocco.

<sup>5</sup>Medicinal Chemistry Laboratory, Faculty of Medicine and Pharmacy, Mohammed V University Rabat, 10170 Rabat, Morocco

<sup>6</sup>National Laboratory for Drug Control, Al Irfane Rabat Morocco

Received 08 Nov 2014,  
Revised 25 Oct 2016,  
Accepted 26 Oct 2016

### Keywords

- ✓ Organo-bentonite;
- ✓ Triazolopyrimidine,
- ✓ carbon steel,
- ✓ Corrosion,
- ✓ inhibition efficiency,
- ✓ EIS.

[youness.chimie14@gmail.com](mailto:youness.chimie14@gmail.com)  
Phone: +212 6 7728 8857

### Abstract

The effect of a prepared compounds, namely 5-methyl[1,2,4]triazolo[1,5-a]pyrimidin-7-ol (MTP) on the corrosion of C-steel in 1M HCl solutions has been studied using the potentiodynamic polarization and electrochemical impedance spectroscopy (EIS) techniques. The results showed that the inhibition efficiency of the investigated compounds was found to depend on the concentration and the nature of the inhibitor. Maximum inhibition efficiency of 94.4% has been achieved using  $10^{-3}$ M of MTP inhibitor. Polarization results indicated that this compound behave as mixed type inhibitor. The adsorption of this compound on steel surface followed Langmuir adsorption isotherm. The reactivity of investigated compounds was analyzed through quantum chemical by DFT method to explain the efficiency of this inhibitor as corrosion inhibitor. The Optical microscope (OM) results showed the formation of a protective film on the metal surface in the presence of this additive.

## 1. Introduction

Studies on preventing the corrosion of steel in acidic environments and the problematic chemical processes that arise have attracted the attention of researchers from a wide range of industrial sectors [1]. Corrosion is the deterioration of metal by chemical attack or reaction with its environment. It is a constant and continuous problem, often difficult to eliminate completely [2].

Preventing the corrosion of steel has played an important role in various industries, especially in the chemical and petrochemical processing industries that employ the use of steel. A number of studies have been conducted to investigate effective methods for preventing corrosion. Acids are widely used in industrial processes, such as pickling, cleaning, descaling, etc. Corrosion inhibitors are used to prevent metal dissolution [3-12]. The corrosion inhibition efficiency of organic compounds is related to their adsorption properties. Adsorption depends on the nature and the state of the metal surface, on the type of corrosive medium and on the chemical structure of the inhibitor [13].

Studies report that the adsorption of the organic inhibitors mainly depends on some physico-chemical properties of the molecule related to its functional group, to the possible steric effects and electronic density of donor atoms; adsorption is also supposed to depend on the possible interaction of  $\pi$ -orbitals of the inhibitor with d-orbitals of the surface atoms, which induce greater adsorption of the inhibitor molecules onto the surface of C-steel, leading to the formation of corrosion protecting film [12-15].

Quantum chemical calculations have been widely used to study the reaction mechanism and to interpret the experimental results as well as to solve chemical ambiguities. This is a useful approach to investigate the

reaction mechanism of the inhibitor molecule and the metal surface. The structural and electronic parameters of the inhibitor molecule can be obtained by means of theoretical calculations using the computational methodologies of quantum chemistry [16].

The present work was designed to study the corrosion inhibition of C-steel in 1M HCl solutions by new Triazole derivative as corrosion inhibitor using different electrochemical techniques. Theoretical calculations have been used to make the correlation between the effectiveness of inhibition of our studied inhibitor and their molecular structure. The chemical structure of the studied compound is given in Fig 1.

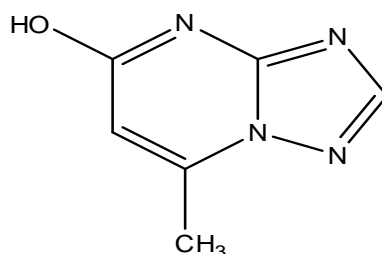


**Figure1:** 5-methyl[1,2,4]triazolo[1,5-a]pyrimidin-7-ol (MTP).

## 2. Experimental

### 2.1. Materials

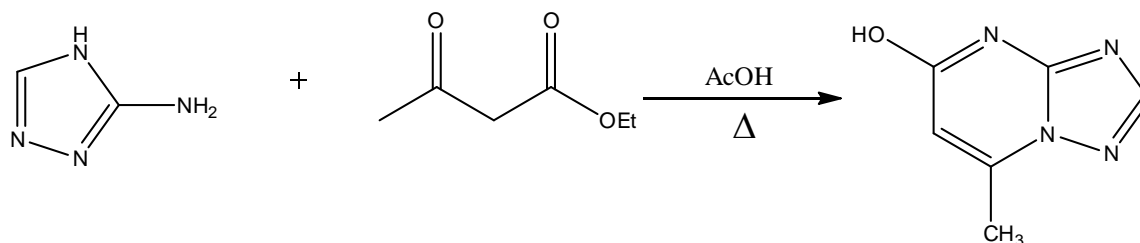
The steel used in this study is a carbon steel (CS) with a chemical composition (in wt%) of 0.370 % C, 0.230 % Si, 0.680 % Mn, 0.016 % S, 0.077 % Cr, 0.011 % Ti, 0.059 % Ni, 0.009 % Co, 0.160 % Cu and the remainder iron Fe.

The specimen was used for electrochemical measurements. The exposed surface area was  $1\text{cm}^2$ .

### 2.2. Solutions

The aggressive solutions of 1M HCl were prepared by dilution of an analytical grade 37% HCl with double distilled water. The concentration ranges of inhibitor employed was  $10^{-5} - 10^{-3}$  (mol/l).

### 2.3. Synthesis of inhibitors



Synthesis of 5-methyl[1,2,4]triazolo[1,5-a]pyrimidin-7-ol.

The compound was characterized by N.M.R.  $^1\text{H-NMR}$  (DMSO- $d_6$ ) ( $\delta$  ppm): 10.47(s,1H,-NH), 6.34(s,1H,HC=), (s,1H,CH<sub>3</sub>), 7.27(s,1H,C=N) .  $^{13}\text{C-NMR}$  (DMSO- $d_6$ ) ( $\delta$  ppm):17.15(-CH<sub>3</sub>), 106.33(HC=), 149.03(C=N), 144.93(C=C), 164.53(C=O), 168.01(C=N)

### 2.4. Electrochemical tests

#### 2.4.1 Electrochemical impedance spectroscopy

The electrochemical measurements were carried out using Volta lab (Tacussel- Radiometer PGZ 301) potentiostat and controlled by Tacussel corrosion analysis software model (Volta master 4) at under static condition. The corrosion cell used had three electrodes. The reference electrode was a saturated calomel electrode (SCE). A platinum electrode was used as auxiliary electrode of surface area of  $1\text{cm}^2$ . The working electrode was carbon steel. All potentials given in this study were referred to this reference electrode. The working electrode was immersed in test solution for  $\frac{1}{2}$  hours to a establish steady state open circuit potential ( $E_{\text{ocp}}$ ). After measuring the  $E_{\text{ocp}}$ , the electrochemical measurements were performed. All electrochemical tests have been performed in aerated solutions at 303 K. The EIS experiments were conducted in the frequency range with high limit of 100 KHz and different low limit 10 mHz at open circuit potential, with 10 points per decade, at the rest potential, after 30 min of acid immersion, by applying 10 mV ac voltage peak-to-peak. Nyquist plots

were made from these experiments and the impedance plots are given in the Nyquist representation. Experiments are repeated three times to ensure the reproducibility.

#### 2.4.2. Potentiodynamic polarization

The electrochemical behavior of carbon steel sample in inhibited and uninhibited solution was studied by recording anodic and cathodic potentiodynamic polarization curves. Measurements were performed in the 1M HCl solution containing different concentrations of the tested inhibitor by changing the electrode potential automatically from -800 to 0 mV versus corrosion potential at a scan rate of 1 mV/s. The linear Tafel segments of anodic and cathodic curves were extrapolated to corrosion potential to obtain corrosion current densities ( $I_{\text{corr}}$ ).

#### 2.4.3. Quantum chemical study

The quantum theoretical calculations were carried out with the Gaussian 09 program package [17]. The complete geometry optimization of the undertaken MTP as corrosion inhibitor was carried out at DFT (Density Functional Theory) using the hybrid functional B3LYP level taking into account the exchange and the correlation with Beck's three parameters exchange functional along with Lee and al. non-local correlation functional [18,19]. All Calculations of DFT/B3LYP theory were done using 6-31G (d,p) basis set.

#### 2.4.4 Morphology of the Carbon steel surface

Immersion corrosion analysis of Carbon steel specimen in the acidic solutions with and without inhibitor was carried out using Optical microscopy (OM). After the corrosion tests, the samples were submitted to OM studies to know the surface morphology.

### 3. Results and discussion

#### 3.1. Potentiodynamic polarization curves

##### 3.1.1. Effect of concentration

Figure 2 shows typical polarization curves for C-steel in 1M HCl media. Various corrosion parameters such as corrosion potential ( $E_{\text{corr}}$ ), cathodic Tafel slopes ( $\beta_c$ ), the corrosion current density ( $I_{\text{corr}}$ ), the degree of surface coverage ( $\theta$ ) and the inhibition efficiency (IE%) are given in Table 1. It can see from the experimental results that in all cases, addition of MTP induced a significant decrease in cathodic and anodic currents.

The slopes of Tafel lines were slightly changed (Tafel lines are parallel) on increasing the concentration of the tested compounds, this indicates a modification of the mechanism of cathodic hydrogen evolution as well as anodic dissolution of steel, which suggest that inhibitor powerfully inhibits the corrosion process of carbon steel, and its ability as corrosion inhibitor is enhanced as its concentration is increased.

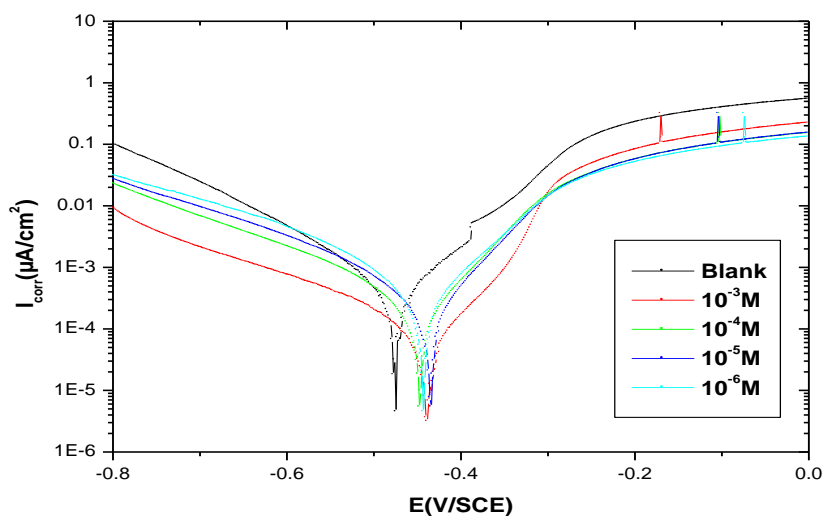


**Figure 2:** Potentiodynamic polarization curves of C-steel in 1M HCl in the presence of different concentrations of MTP at 303K.

It's clear from this figure that the addition of the inhibitor concentration causes a significant decrease in the corrosion rate, a displacement of the anodic curves to more positive potentials and the cathodic curves to more negative potentials. This may be attributed to adsorption of the inhibitor on the electrode surface. The inhibition efficiency values  $IE$  (%), were calculated using the following equation (1):

$$IE \% = \frac{I_{corr}^{\circ} - I_{corr}}{I_{corr}^{\circ}} \times 100 \quad (1)$$

Where  $I_{corr}^{\circ}$  and  $I_{corr}$  are uninhibited and inhibited corrosion current densities, respectively.

From Table 1, it is clear that increasing concentration of the inhibitor resulted in a decrease in corrosion current densities ( $I_{corr}$ ) and an increase in inhibition efficiency ( $IE$  %), reaching its maximum value 94.4% at  $10^{-3}M$ . This behavior suggests that the inhibitor adsorption protective film formed on the carbon steel surface tends to be more and more complete and stable. The presence of MTP derivative caused a slight shift of corrosion potential towards the positive values compared to that in the absence of inhibitor. In literature, it has been also reported that if the displacement in  $E_{corr}$  is  $> 85$  mV the inhibitor can be seen as a cathodic or anodic type inhibitor and if the displacement of  $E_{corr}$  is  $< 85$  mV, the inhibitor can be seen as mixed type [20]. In our study, the maximum displacement in  $E_{corr}$  value was less than 85 mV for MTP derivative which indicates that the inhibitor acts as mixed type inhibitor with predominantly control of anodic reaction.

**Table 1:** Electrochemical parameters of C-steel in 1M HCl solution without and with MTP derivative.

Medium	Conc (M)	$-E_{corr}$ (mV <sub>SCE</sub> )	$-\beta_c$ (mV dec <sup>-1</sup> )	$I_{corr}$ ( $\mu A$ cm <sup>-2</sup> )	$IE$ (%)	$\theta$
HCl	1	441.0	138	579	—	—
MTP	$10^{-3}$	449.7	89.7	32.4	94.4	0.944
	$10^{-4}$	448.8	88.3	99.6	82.7	0.827
	$10^{-5}$	456.0	91.4	155.7	73.1	0.731
	$10^{-6}$	432.0	92.0	189.6	67.2	0.672

### 3.1.2. Effect of temperature

The effect of temperature on both corrosion and corrosion inhibition of carbon steel in 1M HCl solution in the absence and presence of different concentrations of investigated compound at different temperatures ranging from 303 to 333K was studied using potentiodynamic measurement, as shown in Table 2.

**Table 2:** various corrosion parameters for C-steel in 1M HCl in absence and presence of optimum concentration of MTP derivatives at different temperatures.

Temperature (K)	$I_{corr}$ ( $\mu A/cm^2$ )		$IE$ (%)
	1M HCl	MTP	
303	579	32	94.7
313	694	130	81.2
323	2026	400	80.2
333	2102	749	64.3

The corrosion rate increases with increasing temperature both in uninhibited and inhibited acid. The apparent activation energy ( $E_a$ ) for the corrosion process can be calculated from Arrhenius-type equation (2)

$$I_{corr} = A \exp\left(-\frac{E_a}{RT}\right) \quad (2)$$

where  $E_a$  is the apparent activation corrosion energy,  $A$  is the Arrhenius pre-exponential factor,  $T$  is the absolute temperature, and  $R$  is the universal gas constant.

The logarithm of the corrosion current density versus  $1000/T$  and the activation energy ( $E_a$ ) values can be calculated from the Arrhenius slope (Fig. 3). The calculated values of the apparent activation corrosion energy in the absence and presence of MTP are listed in Table 3.

The alternative formulation of transition state equation is shown in eq (3):

$$I_{corr} = \frac{RT}{Nh} \exp\left(\frac{\Delta S_a}{R}\right) \exp\left(\frac{\Delta H_a}{RT}\right) \quad (3)$$

Where T the absolute temperature, h the Planck's constant, N the Avogadro's number,  $\Delta S_a$  the entropy of activation,  $\Delta H_a$  the enthalpy of activation and  $I_{corr}$  is the corrosion rate.

The plots of  $\ln(I_{corr}/T)$  versus  $1000/T$  (Fig. 4) show almost straight lines and all the regression coefficients are close to 1. From the slopes and intercepts of the straight lines, the values of  $\Delta H_a$  and  $\Delta S_a$  were calculated and listed in Table 3.

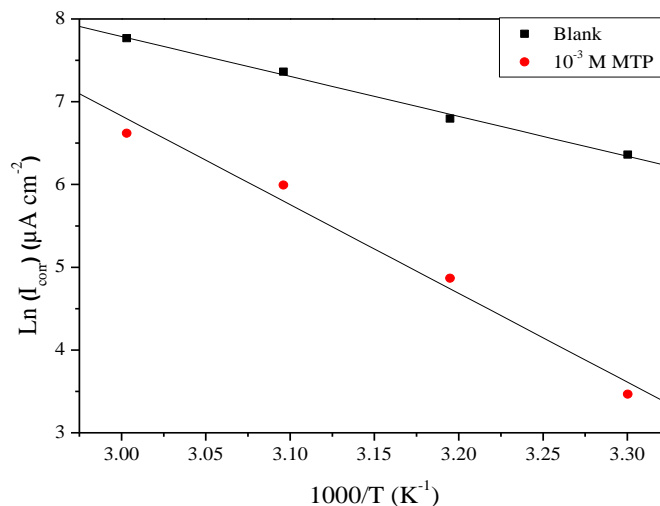


**Figure 3:** Arrhenius plots of C-steel in 1M HCl with and without  $10^{-3}$  M of MTP derivatives.

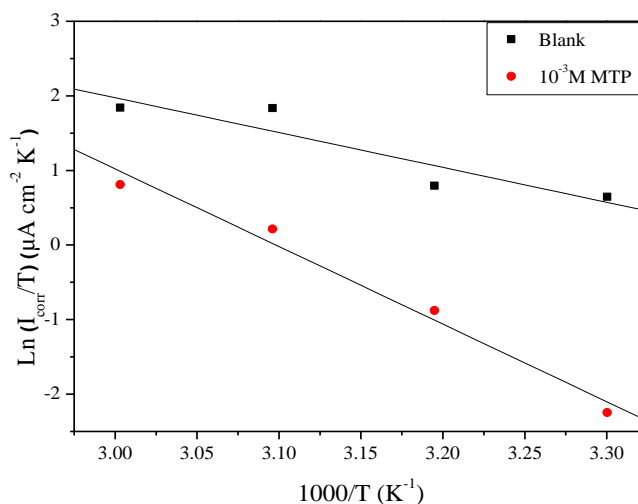


**Figure 4:** Arrhenius plots of  $\ln I_{corr}/T$  vs.  $1/T$  for steel in 1M HCl in the absence and the presence of MTP at optimum concentration.

**Table 3:** Activation parameters for the steel dissolution in 1M HCl in the absence and the presence of MTP at optimum concentration.

Medium	Linear regression coefficient (r)	$E_a$ (kJ/mol)	$\Delta H_a$ (kJ mol <sup>-1</sup> )	$\Delta S_a$ (J mol <sup>-1</sup> K <sup>-1</sup> )
HCl	0.97625	40.12	38.84	-64.59
MTP	0.99764	89.14	86.50	70.45

The increase of the  $E_a$  with increase inhibitor concentration Table 3 is typical of physical adsorption. This means the presence of the inhibitor induces an energy barrier for corrosion reaction and the barrier increases with increasing concentration. At higher temperatures, there is an appreciable decrease in the adsorption of the inhibitor on the metal surface and a corresponding rise in the corrosion rate occurred [21].

The positive shift of enthalpy of activation ( $\Delta H_a$ ) with the presence of inhibitor concentration reflects that the process of adsorption of the inhibitor on the C-S surface is an endothermic process [21]. In the absence of MTP for carbon steel the large negative value of a  $\Delta S_a$  implies that the activated complex is the rate determining step, rather than the dissociation step. In the presence of the inhibitor, the values of a  $\Delta S_a$  increases and is generally interpreted as an increase in disorder as the reactants are converted to the activated complexes, simply the disorder increases with MTP [22]. The positive values of  $\Delta S_a$  reflect the fact that the adsorption process is accompanied by an increase in entropy, which is the driving force for the adsorption of the inhibitor onto the steel surface.

### 3.1.3. Adsorption isotherm

One of the most convenient ways of expressing adsorption quantitatively is by deriving the adsorption isotherm that characterizes the metal/inhibitor/ environment system. Various adsorption isotherms were applied to fit  $\theta$  values but the best fit was found to obey Langmuir adsorption isotherm which are represented in Figure1 for investigated MTP inhibitor, Langmuir adsorption isotherm may be expressed by:

$$\frac{C}{\theta} = \frac{1}{K_{ads}} + C \quad (4)$$

Where  $C$  is the concentration ( $\text{mol.L}^{-1}$ ) of the inhibitor in the bulk electrolyte,  $\theta$  is the degree of surface coverage ( $\theta = \% \text{IE}/100$ ),  $K_{ads}$  is the adsorption equilibrium constant.

A plot of  $C$  versus  $C/\theta$  should give straight line. In order to get a comparative view, the variation of the adsorption equilibrium constant ( $K_{ads}$ ) of the inhibitor with their molar concentrations was calculated. The experimental data give good curves fitting for the applied adsorption isotherm as the correlation coefficients ( $R^2 = 0.9998$ ) (Fig. 5). The values obtained are given in Table 4. The extent of inhibition is directly related to the performance of adsorption layer which is a sensitive function of the molecular structure. The equilibrium constant of adsorption  $K_{ads}$  obtained from the intercepts of Langmuir adsorption isotherm is related to the free energy of adsorption  $\Delta G_{ads}^\circ$  as follows:

$$\Delta G_{ads}^\circ = -RT \ln(55.5 K_{ads}) \quad (5)$$

Where 55.5 mol/L is the molar concentration of water.

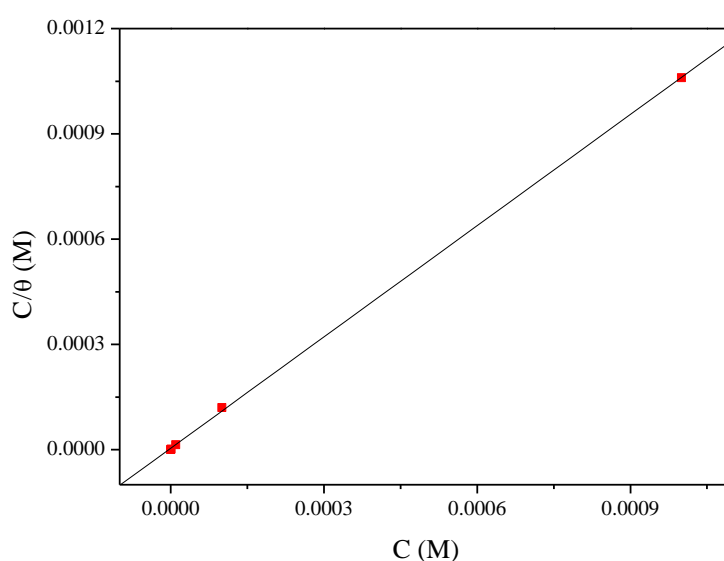


**Figure 5:** Langmuir adsorption isotherm of MTP derivatives on the C-steel surface in HCl solution

The negative sign of  $\Delta G_{\text{ads}}^{\circ}$  indicates the spontaneity of the adsorption process and stability of the adsorbed film on the electrode surface [23]. Furthermore, values of  $\Delta G_{\text{ads}}^{\circ}$  up to  $-20 \text{ kJ}\cdot\text{mol}^{-1}$  are reliable with the electrostatic interaction between the charged molecules and the charged metal (physisorption) while those more negative than  $-40 \text{ kJ}\cdot\text{mol}^{-1}$  involve sharing or transfer of electrons from the inhibitor molecules to the metal surface to form a co-ordinate type of bond (chemisorption) [24-26]. Accordingly, the value of  $\Delta G_{\text{ads}}^{\circ} = -43.8 \text{ kJ/mol}$  we propose chemisorption of MTP molecules on the C-steel surface. In fact, because of strong adsorption of  $\text{H}_2\text{O}$  molecules on the surface of steel, it may be assumed that removal of water molecules from the surface is accompanied by chemical interaction between the metal surface and the formed film [27].

**Table 4:** Thermodynamic parameters for the corrosion of C-steel in 1M HCl in the absence and presence of MTP.

	$R^2$	Slope	$K_{\text{ads}} (\text{M}^{-1})$	$\Delta G_{\text{ads}}^{\circ} (\text{KJ mol}^{-1})$
MTP	0.99988	1.05	237021.05	-41.3

### 3.2. Electrochemical impedance spectroscopy (EIS)

The Electrochemical impedance spectroscopy is powerful technique for studying the corrosion. Surface properties, electrode kinetics and mechanistic information can be obtained from impedance diagrams [28]. Figure 6 shows the Nyquist plots obtained at open-circuit potential in the absence and presence of increasing concentrations of investigated compounds at 303 K. The increase in the size of the capacitive loop with the addition of investigated compound shows that a barrier gradually forms on the C-steel surface. The increase in the capacitive loop size (Figure 6) enhances, confirming the highest inhibitive influence of MTP compound. Obviously correlating with the increase of inhibitor adsorbed on C-steel surface. The deviation from ideal semicircle was generally attributed to the frequency dispersion [28] as well as to the inhomogeneity of the surface.

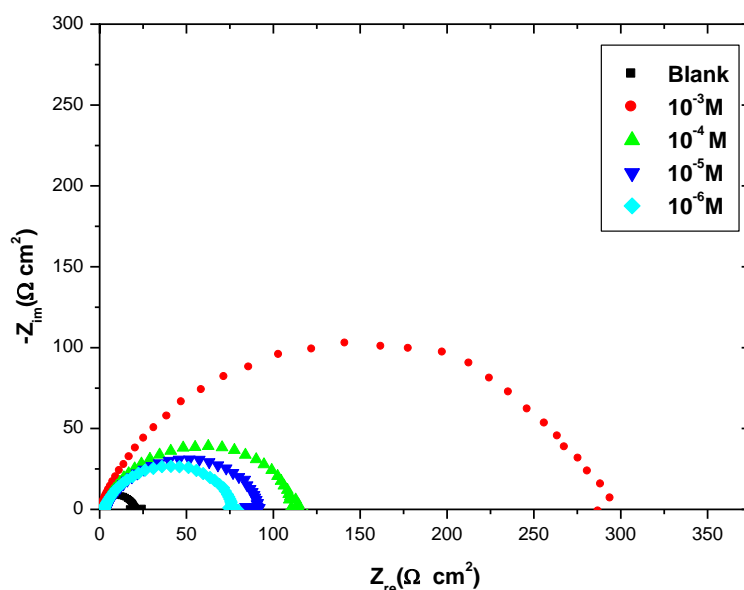


**Figure 6:** Nyquist plots for C- steel in 1M HCl containing different concentrations of MTP.

EIS spectra of the investigated MTP compound was analyzed using the equivalent circuit, Figure 7, which represents a single charge transfer reaction and fits well with our experimental results. The constant phase element, CPE, is introduced in the circuit instead of a pure double layer capacitor to give a more accurate fit [29]. The double layer capacitance,  $C_{dl}$ , for a circuit including a CPE parameter ( $Y_0$  and  $n$ ) were calculated from eq.6 [29]:

$$C_{dl} = \frac{1}{2\pi f_m R_t} \quad (6)$$

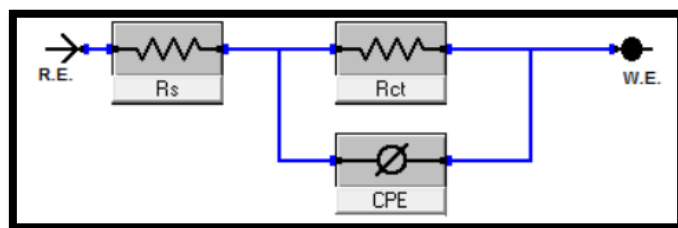


**Figure 7:** Equivalent circuit used to fit the impedance spectra.

Where  $Y_0$  is the magnitude of the CPE,  $\omega_{\max} = 2\pi f_{\max}$ ,  $f_{\max}$  is the frequency at which the imaginary component of the impedance is maximal and the factor  $n$  is an adjustable parameter that usually lies between 0.50 and 1.0. After analyzing the shape of the Nyquist plots, it is concluded that the curves approximated by a single capacitive semicircles, showing that the corrosion process was mainly charged-transfer controlled [30,31]. The general shape of the curves is very similar for all samples indicating that no change in the corrosion mechanism [32]. From the impedance data Table 5, we concluded that the value of  $R_{ct}$  increases with increasing the concentration of the inhibitor and this indicates an increase in  $\% \eta_z$ .

**Table 5:** AC impedance data of C-steel in 1M HCl acid solution containing different concentrations of MTP at 303K.

Medium	Conc (M)	$R_{ct}$ ( $\Omega \text{ cm}^2$ )	$C_{dl}$ ( $\mu\text{F}/\text{cm}^2$ )	$f_{\max}$ (Hz)	$\eta_z$ (%)
HCl	1	20	199	40	—
MTP	$10^{-3}$	314	62.7	8	93.0
	$10^{-4}$	115	110.7	12.5	85.6
	$10^{-5}$	92	109.4	15.82	78.2
	$10^{-6}$	77	165.4	12.5	74.0

In fact, the presence of inhibitor enhances the value of  $R_{ct}$  in acidic solution. Values of double layer capacitance are also brought down to the maximum extent in the presence of inhibitor and the decrease in the values of CPE follows the order similar to that obtained for  $I_{\text{corr}}$  in this study. The decrease in  $\text{CPE}/C_{dl}$  results from a decrease in local dielectric constant and/or an increase in the thickness of the double layer, suggesting that organic derivatives inhibit the C-steel corrosion by adsorption at metal/acid [33,34]. The inhibition efficiency was calculated from the charge transfer resistance data from Eq.7 [35]:

$$\eta_z \% = \frac{R_{ct}^i - R_{ct}^{\circ}}{R_{ct}^i} \times 100 \quad (7)$$

Where,  $R_{ct}^{\circ}$  and  $R_{ct}^i$  are the charge transfer resistance in absence and in presence of inhibitor, respectively.

### 3.3. Quantum chemical calculations

To investigate the effect of molecular structure on the inhibition mechanism and inhibition efficiency, some quantum chemical calculations were performed. Quantum chemical parameters such as the energy of highest occupied molecular orbital ( $E_{\text{HOMO}}$ ), the energy of the lowest unoccupied molecular orbital ( $E_{\text{LUMO}}$ ), HOMO – LUMO energy gap ( $\Delta E_{\text{gap}}$ ), the dipole moment ( $\mu$ ) of optimized molecular and protonated (N-MTP) structures of the inhibitor MTP (Figures. 8 and 9 had been calculated (Table 6).

Frontier molecular orbital theory suggests that the formation of a transition state is due to an interaction between frontier orbitals (HOMO and LUMO) of reacting species. It is well-known that low absolute values of the energy band gap gives good inhibition efficiencies, because the ionization potential will be low [36]. The dipole moment ( $\mu$ ) is a measure of the polarity of a covalent bond, which is related to the distribution of electrons in a molecule [37]. Although literature is inconsistent with the use of  $\mu$  as a predictor for the direction of a corrosion inhibition reaction, it is generally agreed that the large values of  $\mu$  favor the adsorption of inhibitor [38]. As it is shown in Table 6, the inhibitor protonated N-MTP has a low  $\Delta E_{\text{gap}}$  (0.19541 eV), which implies the high ability to accept electrons from the d-orbital of Fe and a high stability of the [Fe-MTP] complexes [39, 40].

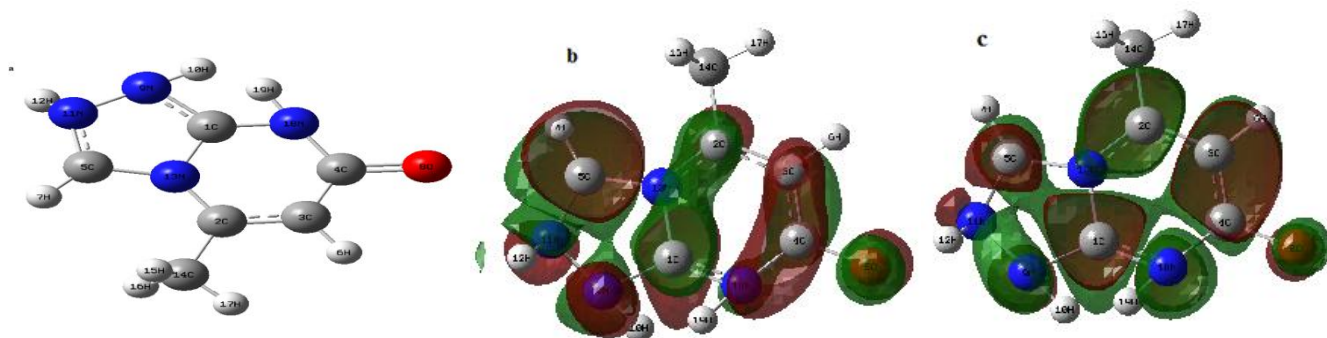


**Figure 8:** Optimized molecular structures of structure MTP(a), HOMO (b), LUMO (c) orbitals.

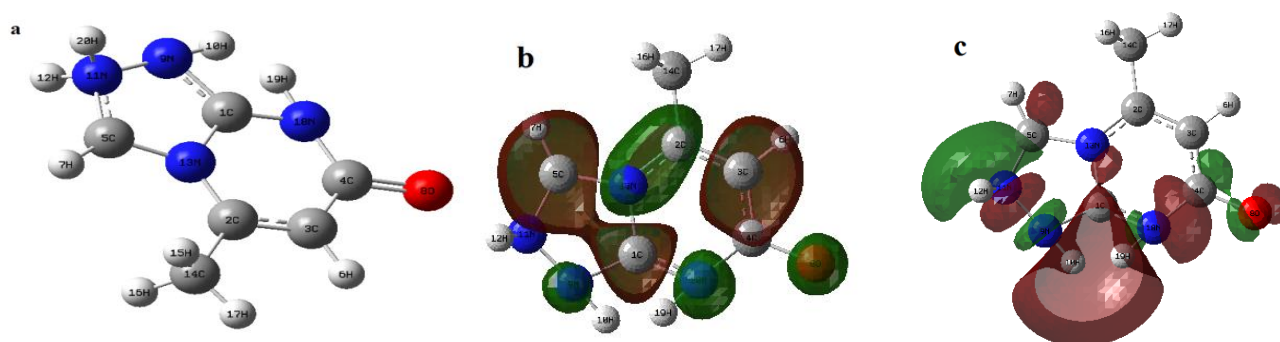


**Figure 9:** Optimized molecular structures of protonated structure (N-MTP(a), HOMO (b), LUMO (c) orbitals.

**Table 6:** Quantum chemical parameters of the studied inhibitor MTP derivative

Molecule	$\mu$ (Debye)	$E_{\text{HOMO}}$ (eV)	$E_{\text{LUMO}}$ (eV)	$\Delta E_{\text{gap}}$ (eV)
MTP	4.5804	-0.25161	-0.04828	0.20333
N-MTP	10.7399	-0.25394	-0.05853	0.19541

Moreover, N-MTP has a rather high value of  $\mu$  (10.7399 D), which implies the strong adsorption of molecule at the carbon steel surface. The Low value of dipole moment of protonated MTP molecule in comparison to protonated N-MTP may decrease the dipole–dipole interaction of molecules and metal surface.

It should be noted that MTP adsorb mainly through electrostatic interactions between the negatively charged nitrogen and carbon atoms and the positively charged metal surface (physisorption). The protonated Structure (Figure. 9) is probably occurred in the acidic medium so some of the protonated nitrogen molecules may attract the other inhibitor molecules with interaction between the molecular nitrogen (chemisorption), in this way the accumulation may occur on the surface. As for the optimized structure, the non-planar structure of MTP molecule diminishes the contact area between MTP molecule and carbon steel surface, while the higher negative charges of N atoms seem beneficial to the adsorption. We can see also from quantum parameters that the adsorption of MTP can involve.

### 3.4. Surface Examinations

Figure 10(a) shows surface morphology of C-steel test coupon before immersion in HCl solution. Some scratches can be noticed on the surface, which are the results of grinding of the C-steel surface with emery paper. Further Test coupon was immersed in 1 M HCl solution for 48 hours and surface morphology was captured (Figure 10(b)). Hydrochloric acid interacted with C-steel aggressively and drastic change in surface morphology of C-steel was observed in comparison to morphology of test sample (Figure 10(a)). In contrast, a smooth and pits free surface can be seen in (Figure10(c)) reflecting retarded steel corrosion in presence of MTP derivative inhibitor. On the basis of micrographs obtained for C-steel, it can be concluded that MTP inhibited C-steel dissolution in acid by covering the surface area with protective film which was found absent in case of acid interaction with steel.

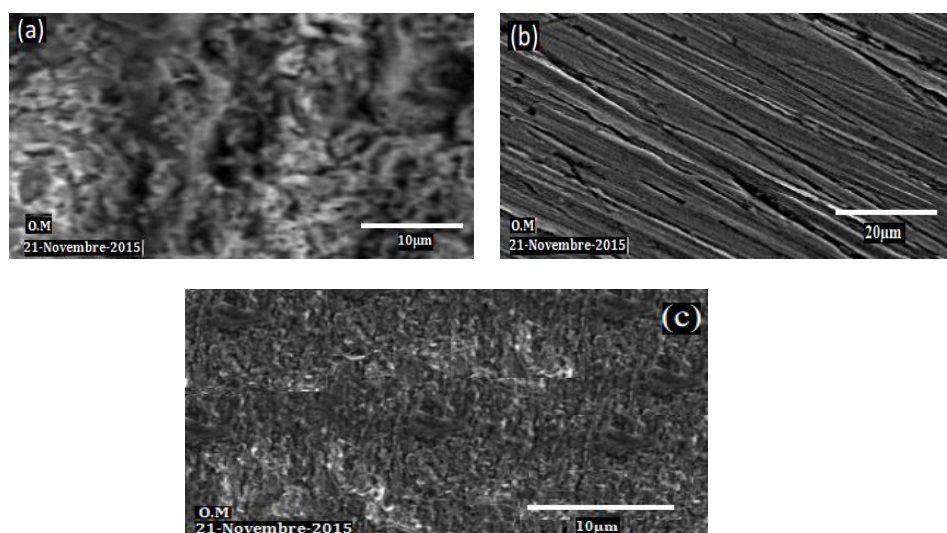


**Figure 10:** O.M of C-steel surface (a) before of immersion in 1M HCl, (b) after 48 h of immersion in 1M HCl , (c) after 48 h of immersion in 1M HCl+  $10^{-3}$  M of MTP.

### Conclusions

5-methyl[1,2,4]triazolo[1,5-a]pyrimidin-7-ol (MTP) was found to be an inhibitor for the corrosion of carbon steel in HCl solution. Inhibition efficiency increases with increase in MTP concentration, but decrease with increase in temperature. Double-layer capacitances decrease with respect to blank solution when the synthesized inhibitor is added. This fact can be explained by adsorption of the synthesized inhibitor species on the steel surface. Polarization studies reveal that MTP act as a mixed-type inhibitor. The adsorption MTP on carbon steel surface can be approximated by Langmuir isotherm model. Quantum chemical parameters for this investigated compound were calculated to provide further insight into the mechanism of MTP inhibition of the corrosion process.

### References

1. Rani B.E.A., Basu B.B.J., Green inhibitors for corrosion protection of metals and alloys: An overview. *Int. J. Corros.* 2012 (2012) 15.
2. Rani B. E. A., Basu B. B. J., *International Journal of Corrosion.* 1 (2012) 1.
3. Zarrok H., Oudda H., El Midaoui A., Zarrouk A., Hammouti B., Ebn Touhami M., Attayibat A., Radi S., Touzani R., *Res. Chem. Intermed.* 38 (2012) 2051.
4. Zarrouk A., Hammouti B., Zarrok H., Bouachrine M., Khaled K.F., Al-Deyab S.S., *Int. J. Electrochem. Sci.* 6 (2012) 89.
5. Zarrouk A., Hammouti B., Dafali A., Zarrok H., *Der Pharm. Chem.* 3 (4) (2011) 266.
6. Zarrok H., Zarrouk A., Salghi, R., Oudda H., Hammouti B., Assouag M., Taleb M., Ebn Touhami M., Bouachrine M., Boukhris S., *J. Chem. Pharm. Res.* 4 (2012) 5056.
7. Ghazoui A., Zarrouk A., Benaft N., Salghi R., Assouag M., El Hezzat M., Guenbour A., Hammouti B., *J. Chem. Pharm. Res.* 6 (2014) 704
8. Zarrok H., Zarrouk A., Salghi R., Assouag M., Hammouti B., Oudda H., Boukhris S., Al Deyab S.S., Warad I., *Der Pharm. Lett.* 5 (2013) 43.
9. Belayachi M., Serrar H., Zarrok H., El Assyry A., Zarrouk A., Oudda H., Boukhris S., Hammouti B., Ebenso Eno E., Geunbour A., *Int. J. Electrochem. Sci.* 10 (2015) 3010.
10. Zarrouk A., Zarrok H., Salghi R., Tourir R., Hammouti, B., Benchat N., Afrine L.L., Hannache H., El Hezzat M., Bouachrine M., *J. Chem. Pharm. Res.* 5 (2013) 1482.
11. Zarrok H., Zarrouk A., Salghi R., Ebn Touhami M., Oudda H., Hammouti B., Tourir R., Bentiss F., Al-Deyab S.S., *Int. J. Electrochem. Sci.* 8 (2013) 6014.
12. Boudalia M., Bellaouchou, A., Guenbour A., Laqhaili A., Mossaddak M., Hammouti B., Ebenso E.E., *Int. J. Electrochem. Sci.*, 8 (2013) 7414.
13. Harmaoui A., El Fal M., Boudalia M., Tabyaouib M., Guenbour A., Bellaouchou A., Ramli Y., Essassi E. M., *J. Mater. Environ. Sci.* 6 (9) (2015) 2509-2519.

14. Boudalia M., Bellaouchou A., Guenbour A., Bourazmi, H., Tabiyaoui, M., El Fal, M., Ramli, Y., Essassi, E.M., Elmsellem H., *Mor. J. Chem.* 2 (2014) 97.
15. Bentiss F., Traisnel, M., Lagrenée M. *J. Appl. Electrochem.*, vol. 31(2001) 41-48.
16. Growcock, F. B., Lopp, V. R., Pomelli, J.W., Ochterski, P.Y., AyalaMorokuma, K., Voth, G.A., Salvador, P., Dannenberg, J.J., Zakrzewski, V.G., Dapprich, S., Daniels, A.D., Strain, M.C., Farkas, O., Malick, D.K., Rabuck, A.D., Raghavachari K., Foresman J.B., Ortiz J.V., Cui Q., Baboul A.G., Clifford S., Cioslowski J., Stefanov, B.B., Liu G., Liashenko, A., Piskorz, P., Komaromi, I., Martin, R.L., Fox, D.J., Keith, T., Al-Laham, M.A., Peng, C.Y., Nanayakkara, A., Challacombe M., Gill P.M.W., Johnson B., Chen W., Wong M.W., Gonzalez C., Pople J.A., Gaussian 03, Revision C.02, Gaussian Inc., Pittsburgh, PA, 2003. *Corros. Sci.* 28 (1988) 397-410.
17. Frisch M.J., Trucks H.B., Schlegel G.E., Scuseria M.A., Robb, J.R. Cheeseman, J.A. Montgomery Jr., T. Vreven, Kudin, K.N., Burant J.C., Millam, J.M., Iyengar, S.S., Tomasi, J., Barone, V., Mennucci, M. Cossi, G. Scalmani, N. Rega, G.A. Petersson, H. Nakatsuji, M. Hada, M. Ehara, K. Toyota, R. Fukuda B., Hasegawa, J., Ishida M., Nakajima, T., Honda, Y., Kitao, O., Nakai, H., Klene, M., Li X., Knox, J.E., Hratchian, H.P., Cross, J.B., Adamo, C., Jaramillo, J., Gomperts, R., Stratmann, R.E., Yazyev, O., Austin, A.J., Cammi, R., C. 870 H. Ju et al. *Corrosion Science.* 50 (2008) 871.
18. Becke D., *J. Chem. Phys.* 98 (1993) 1372.
19. Lee C., Yang W., Parr, R.G., *Phys. Rev.* 37B (1988) 785.
20. Milton H.L., Eloisa A. H., Guilherme J. M., *Flav. Fragr. J.* 20 (2005) 462.
21. Boudalia M., Sebbar N.K., Lahmidi S., Ouzidan Y., Essassi E.M., Tayebi H., Bellaouchou A., Guenbour A., Zarrrouk A., *J. Mater. Environ. Sci.* 7 (3) (2016) 888.
22. El Ouali I., Hammouti B., Aouniti A., Ramli Y., Azougagh M. Essassi E.M., Bouachrine M., *J. Mater. Environ. Sci.* 1(1) (2010) 1.
23. Hussin M., Kassim H., *J. Mater. Chem. Phys.* 125 (2011) 461.
24. Lorenz W. J., Mansfeld F., *Corros. Sci.* 21 (1981) 647.
25. Ghazoui A., Benchat N., El-Hajjaji F., Taleb M., Rais Z., Saddik R., Elaattiaoui A., Hammouti B., *Journal of Alloys and Compounds*, 693 (2017) 510-517
26. Yurt A, Bereket G, Kivrak A, Balaban Erk B. *J Appl Electrochem*, 35 (2005) 1025.
27. Sebbar N.K., Elmsellem, H., Boudalia, M., Lahmidi, S., Bellaouchou, A., Guenbour, A., Essassi, E.M., Steli, H., Aouniti A. *J. Mater. Environ. Sci.* 6 (11) (2015) 3044
28. El Achouri M., Kertit S., Gouttaya H.M., Nciri B., Bensouda Y., Perez L., Infante M., Elkacemi K., *Prog. Org. Coat.* 43 (2001) 267.
29. Macdonald J.R., Johanson W.B., in: J.R. Macdonald (Ed.), *Theory in Impedance Spectroscopy*, John Wiley & Sons, New York. 20 (1987) 289-305.
30. Mertens S. F., Xhoffer C., Decooman B. C., Temmerman E., *Corrosion, Sci.* 53 (1997) 381.
31. TrabANELLI G., Montecelli C., Grassi V., Frignani A., *J. Cem. Concr. Res.* 35 (2005) 1804.
32. Trowsdat A.J., Noble B., Haris S.J., Gibbins I.S. R., Thomson G. E., Wood G.C., *Corros. Sci.* 38 (1996) 177
33. Reis F. M., De Melo, H.G., Costa I.; *Electrochim. Acta*, 51 (2006) 17.
34. Lagrenée M., Mernari B., Bouanis M., Traisnel M., Bentiss F., *Corros. Sci.* 44 (2002) 573.
35. Chen H. Ma, S., Niu, L., Zhao S., Li, S., Li, D., *J. Appl. Electrochem.* 32 (2002) 65.
36. Gokhan G., *Corros. Sci.* 50 (2008) 50.
37. El Sayed H., El Ashry, El Nemr A., Esawy, S.A., Ragab S., *Electrochim. Acta* 51(19) (2006) 3957-3968.
38. Eddy N.O., Ita B.I., *J. Mol. Model.* 17(2) (2011) 359.
39. Oguzie E., Enenebeaku C.K., Akalezi C.O., Okoro S.C., Ayuk A.A., Ejike E.N., *J. Colloid Interface Sci.* 1 (2010) 349.
40. EL Arouji S., Alaoui Ismaili K., Zerrouki A., El Kadiri S., El Assry A., Rais Z., Filali M., Taleb M., Zarrrouk A., Aouniti, Hammouti B., *Der Pharma Chemica.* 7(10) (2015) 23.
41. Bouasla, S, Teguiiche, M. *J.Mar. Chim. Heterocycl.* 10(1) (2011) 10.
42. Bentama A, Hamdach A, ElHadrami M, ElHallaoui A, Elachqar A, El Hajji S., *J. Mar. Chim. Heterocycl.* 2 (2002) 1.

(2017) ; <http://www.jmaterenvironsci.com/>